EPJ Web of Conferences **301**, 02006 (2024) https://doi.org/10.1051/epjconf/202430102006
XLV Symposium on Nuclear Physics 2024

Using indirect methods to explore low-energy fusion cross sections in nuclear astrophysics

Marco La Cognata[1,*]

[1]Istituto Nazionale di Fisica Nucleare, Laboratori Nazionali del Sud, 95123 Catania, Italy

Abstract. Nuclear reactions within stellar environments typically manifest at energies well below 1 MeV. As a consequence, the Coulomb barrier strongly suppresses the cross section, diminishing it to values as minute as a few nanobarns for charged particles. This challenge in obtaining precise input data for astrophysics has prompted the utilization of indirect methodologies. Specifically, approaches such as ANC and THM have been employed to ascertain cross sections for reactions involving photons and charged particles in the exit channel, respectively, obviating the necessity for extrapolation. The discourse explores recent findings arising from the application of these methodologies. For example, the measurement of ^{6}Li(^{3}He,d)^{7}Be is employed to infer the ANC's of the ^{3}He+^{4}He→ ^{7}Be and p+^{6}Li→ ^{7}Be channels, along with their corresponding radiative-capture cross sections. Furthermore, the THM measurement of the ^{27}Al$(p,\alpha)^{24}$Mg cross section via the ^{2}H(^{27}Al,α ^{24}Mg)n reaction is emphasized. In both instances, the cross section at astrophysical energies has been ascertained with unparalleled precision.

1 Introduction to indirect methods

Indirect methodologies encompass approaches that facilitate the determination of the astrophysical factor [1] for a reaction by measuring the cross section of a correlated process and employing nuclear reaction theory to establish the correlation. These techniques play a pivotal role in the investigation of nuclear reactions with astrophysical relevance. In the realm of astrophysics, especially during steady-burning phases of stellar evolution, energies of interest are so meager that the Coulomb barrier markedly diminishes cross sections, making direct measurements virtually unfeasible for charged particles. The energies situated within the Gamow window [1], typically spanning from a few keV to several hundred keV, can yield cross sections much smaller than 1 nb, necessitating extrapolation from higher energies. While utilizing the astrophysical factor, a function of energy that varies smoothly, assists in minimizing systematic errors introduced by extrapolation, resonant reactions may deviate significantly from this smooth behavior due to resonances that are unknown or unpredicted. Even in non-resonant cross sections, electron screening introduces uncertainty in extrapolation, as evidenced in specific case studies [2]. Electron screening becomes noteworthy when interaction energies are comparable to electron binding energies in atoms, and the influence of atomic electrons cannot be disregarded. Electron clouds amplify the astrophysical factor by shielding nuclear charges, complicating the assessment of the bare-nucleus cross section,

*e-mail: lacognata@lns.infn.it

a critical aspect for astrophysical applications, with traditional beam and solid or gaseous target reactions. Therefore, indirect methods are indispensable.

This study concentrates on two indirect approaches. Initially, the Asymptotic Normalization coefficient (ANC) technique, particularly suitable for pure external direct capture processes [3], will be examined. Then, the Trojan Horse Method (THM) [4] will be illustrated. The THM has effectively investigated low-energy nuclear reactions induced by charged particles [5, 6], encompassing radioactive ion beams [8] and neutrons [9], utilizing the modified R-matrix theoretical framework for analyzing multi-resonance reactions [10], similarly to the thick-target inverse kinematics approach [7].

1.1 Radiative capture reactions: the ANC approach

The cross section for a $A(a,\gamma)B$ radiative capture reaction can be expressed at low energies through the matrix element $M = \langle \psi_B | O(r_{Aa}) | \psi_A \chi_a \rangle$, where $O(r_{Aa})$ represents the radial component of the electromagnetic multipole operator, dependent on the distance r_{Aa} between the projectile and the target nucleus. The wave functions ψ_A and ψ_B correspond to the initial state of nucleus A and the final state of nucleus B after $a-$capture, while χ_a denotes the wave function of the incident structureless particle a. The matrix element M is proportionate to the $B = A + a$ overlap function; at an asymptotic distance, it can be expressed as the product of the ANC $C_{Aal_Bj_B}$ and the Whittaker function [3]. Thus, in peripheral reactions, where only the outer portion of the nuclear radial integrals contributes to the cross section, the $A(a,\gamma)B$ radiative capture cross section is proportional to the square of the ANC $C_{Aal_Bj_B}$.

A crucial aspect of applying the ANC method is that these ANCs can be determined from transfer reactions such as $A(C,D)B$, where $C = D + a$ is utilized to transfer particle a and populate the B system. For this purpose, the $A(C,D)B$ differential cross sections are calculated using, for instance, the Distorted Wave Born Approximation (DWBA) approach. From the DWBA differential cross section computed at the primary peak of the angular distribution, the relevant ANCs can be inferred as detailed in [11]. Analogous to the THM scenario, the inferred cross sections are immune to electron screening effects and can extend down to zero energy without necessitating extrapolation. Nevertheless, generally, only the direct capture contribution to the overall radiative capture cross section can be established in the ANC framework. Another advantage of the method is that ANC provides the absolute normalization of direct capture cross sections. In numerous instances, theoretical calculations can reproduce the trend of the cross sections but miss the absolute value of the cross sections (and astrophysical factors), underscoring the significance of utilizing ANC.

1.2 Reaction with charged particles or neutrone in the exit channel: the THM method

In the THM, the cross section for the $A(x,b)B$ reaction is obtained via the $A(a,bB)s$ reaction executed at energy levels substantially surpassing astrophysical magnitudes (several tens of MeV versus tens of keV in astrophysics). This guarantees that neither Coulomb nor centrifugal barriers in the entrance channel hinder the cross section, and electron screening does not influence the astrophysical factor at astrophysical energy ranges. To establish a connection between the $A(a,bB)s$ process and the astrophysical $A(x,b)B$ reaction, the quasi-free (QF) condition is imposed, wherein the phase space region is selected based on particles x and s, forming the TH nucleus a, having distances greater than the nuclear interaction radius. This condition corresponds to small $x - s$ relative momenta, below approximately $(2\mu_{xs}B_{xs})^{1/2}$ (where μ_{xs} and B_{xs} denote the reduced mass and binding energy of the $x - s$ system, respectively), and implies that the $A - x$ interaction is unaffected by the presence of s (particularly if

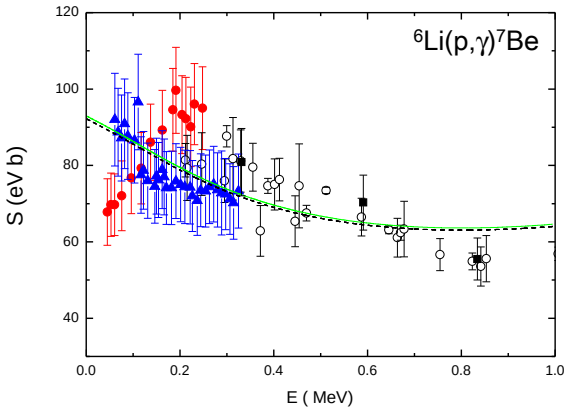

Figure 1. The astrophysical S factor for the ^{6}Li$(p,\gamma)^7$Be radiative-capture reaction is depicted through both experimental and calculated means. The S factor obtained through the application of ANC values derived from near-barrier proton transfer ^{6}Li(^{3}He,d)^{7}Be is represented by the solid green line. The calculated S factor, marked by the black line, is determined from the ANCs derived through a reevaluation of the data presented in ref.[17], illustrated as blue solid triangles. Our findings lean toward challenging the conclusions drawn in ref.[16], with the trend indicated by the green line conflicting with the corresponding data (red solid circles). Conversely, our results align well with the extrapolation from ref.[17], demonstrating a notably improved accuracy (5.9%, accounting for systematic errors). In this representation, black symbols are utilized to denote prior measurements, as discussed in ref.[14].

x or s is a neutron, given the long-range nature of Coulomb interaction). Nevertheless, since particle x is virtual, the astrophysical process $A(x,b)B$ is half-off-energy-shell (HOES), as the particles in the entrance channel all satisfies the mass-shell equation, and a straightforward comparison with the corresponding on-energy-shell (OES) direct process [12] is not possible. To address the intricacies introduced by the HOES nature in the multi-resonance scenario, the modified R-matrix approach is employed to extract the astrophysical S-factor of interest from the QF reaction yield [10].

2 The ^{3}He$(\alpha,\gamma)^7$Be and ^{6}Li$(p,\gamma)^7$Be radiative capture processes

The role of the ^{3}He$(\alpha,\gamma)^7$Be reaction is pivotal in nuclear astrophysics, serving as the initial stage in both the 2^{nd} and 3^{rd} branches of the proton-proton $(p-p)$ chain. The uncertainty in its rate holds significant sway over the projected flux of ^{7}Be and ^{8}B neutrinos. Despite advancements in solar neutrino detection precision facilitated by large detectors, the ^{3}He$(\alpha,\gamma)^7$Be reaction retains its importance, grappling with uncertainties ranging from 5-8%, notably exceeding the requisite 3% precision (refer to ref.[13] for a comprehensive discussion). Employing the ANC approach proves advantageous for scrutinizing the ^{3}He$(\alpha,\gamma)^7$Be astrophysical factor at low energies. At these energy levels, the trends are well-understood, but the absolute values exhibit significant variation, as anticipated in sect.1.1.

In accordance with the discussions in references [13, 14], ANCs for the ^{3}He$(\alpha,\gamma)^7$Be reaction were derived through the investigation of the near-barrier ^{6}Li(^{3}He,d)^{7}Be α particle transfer reaction, particularly at backward angles. This process, characterized as a pure external direct capture at stellar energies [15], displays diminished sensitivity to nuclear structure,

given its occurrence through the tail of the nuclear overlap function. The obtained ANCs facilitated the precise determination of the $S_{34}(0)$ factor as it will shown.

Utilizing the same dataset, with a focus on angular distributions at forward angles, the deduction of the ^{6}Li$(p,\gamma)^7$Be radiative capture cross section was possible (refer to [14] for detailed information). This reaction holds paramount importance in addressing the primordial lithium problem, and an accurate determination of the ^{6}Li$(p,\gamma)^7$Be astrophysical S-factor is indispensable. Nevertheless, existing experimental data present conflicting outcomes, necessitating consideration of the electron screening effect. Recent experiments [17] have cast doubt on the existence of a previously claimed 200 keV resonance in earlier works [16], attributing it to the presence of a $J^\pi = (1/2^+, 3/2^+)$ state in ^{7}Be.

By utilizing ^{3}He beams sourced from the University of Catania (Italy) and the FN tandem accelerator at Florida State University, we conducted measurements of the transfer reaction to derive the ANCs for the ^{3}He+α $\rightarrow^7$Be channel. The analysis adopted the Distorted Wave Born Approximation (DWBA) framework [18], assuming one-step proton and α-particle transfers. The resulting squared ANCs for the ground state and first excited state of ^{7}Be were determined as C^2=20.84 ± 1.12 [0.82; 0.77] fm^{-1} and C^2=12.86 ± 0.50 [0.35; 0.36] fm^{-1}, respectively. The uncertainties encompass both experimental errors on $d\sigma^{\rm exp}/d\Omega$ and the ANC of the d +^{4} He $\rightarrow$ ^{6}Li channel (first term in square brackets), as well as model uncertainties (second term in square brackets). In what follows, we will consistently use this notation, indicating the two components of the errors, statistical and systematic, as the first and second term in square brackets.

Subsequently, within the Modified Two-Body Potential Model (MTBPM) [13, 14], the contribution of direct capture to the ^{3}He(^{4}He,γ)^{7}Be astrophysical factor was determined. The resulting S factors, $S_{34}(0)$ and S_{34}(23 keV), were found to be $S_{34}(0) = 0.534 \pm 0.025$ [0.015; 0.019] keVb and S_{34}(23 keV) = 0.525 ± 0.022 [0.016; 0.016] keVb. A comparison with literature values highlights enhanced accuracy compared to the currently recommended value in ref.[15], although the uncertainty still exceeds the desired level, necessitating further efforts for reduction.

For the ^{6}Li$(p,\gamma)^7$Be system, squared ANCs (C_p^2) and their uncertainties were determined, resulting in $C_p^2 = 4.51 \pm 0.21\,[0.15; 0.15]\,\text{fm}^{-1}$ for the ground state and $C_p^2 = 4.37 \pm 0.44\,[0.31; 0.31]\,\text{fm}^{-1}$ for the first excited state of ^{7}Be. The experimental error includes statistical and normalization errors, while the theoretical uncertainty considers variations in the adopted potential parameters. The ^{6}Li$(p,\gamma)^7$Be S-factor, primarily influenced by $E1$ transitions, was derived within the modified two-body potential model, demonstrating improved accuracy compared to direct measurements [16, 17]. The ANC astrophysical factor is presented in fig. 1 as a green line, alongside available experimental data. Another calculation, depicted as a black line, illustrates the astrophysical factor derived by deducing the ANCs from the data in ref.[17], validating our approach. Quantitatively, the indirect $S_{61}(E)$ equals 90.4±2.4 eV·b for E=0 and 89.2±2.3 eV·b for E= 15.1 keV, in excellent agreement with the extrapolated S-factor to zero energy (S(0) = 95 ± 9 eV·b) in ref.[17], with significantly improved accuracy. The results tend to refute the claimed 200 keV resonance [16] and support a smooth S-factor increase towards zero energy, as evident in fig. 1. It is worth noting that this comparison made it possible to perform an independent test of the procedure to derive the ANCs and the one to calculate the astrophysical factor using the MTBPM.

3 The THM measurement of the ^{27}Al(p,α)^{24}Mg reaction

The THM proves particularly suitable for investigating the ^{27}Al$(p,\alpha)^{24}$Mg reaction at astrophysical energy regimes. This reaction holds significance in various astrophysical contexts

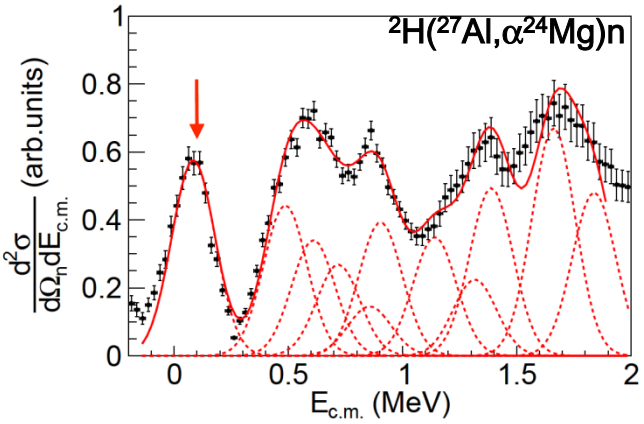

Figure 2. The differential cross section for the ^{2}H(^{27}Al,α^{24}Mg)n reaction is illustrated by the black circles. A fitting procedure, employing equation A5 from ref.[19], yields the red solid line. Dashed lines are incorporated to emphasize the influence of individual resonances. The profile of each peak is established by convolving the theoretical Breit-Wigner shape with the experimental response function, as detailed in ref.[20]. The red arrow denotes the energy region pertinent to astrophysical considerations.

(refer to ref.[20] and associated references). The widely adopted rate for astrophysical predictions, detailed in [24] at $T_9 = 0.1$, provides lower, median, and upper values of 1.85×10^{-11}, 4.34×10^{-11}, and 8.51×10^{-11} cm^3 mol^{-1} s^{-1}, respectively, spanning nearly one order of magnitude. The uncertainty range widens at lower temperatures. The THM has facilitated investigations down to zero energy, providing insights into the energy region of astrophysical interest below approximately 100 keV. In this context, a ^{27}Al projectile was accelerated onto a deuteron target nucleus, which was chosen as Trojan Horse (TH) nucleus for its simple $p+n$ structure, primarily manifesting $p-n$ motion in s-wave [21]. By selecting small $p-n$ relative momenta corresponding to large $p-n$ relative distances, ^{27}Al interacts solely with the proton involved in the TH reaction, with the neutron acting as a spectator. Excited states of ^{28}Si were populated, subsequently decaying into the ^{24}Mg + α channel, selected in the offline analysis. As the beam energy compensates for the deuteron binding energy, the ^{27}Al + p reaction can occur in the energy region of astrophysical relevance.

Fig. 2 depicts the outcome of the THM measurement. As elaborated in ref.[20, 22], where the entire data analysis is expounded, the ^{2}H(^{27}Al, α^{24}Mg)n QF cross section reveals numerous resonances, aligning with expectations from the examination of the ^{27}Al$(p,\alpha)^{24}$Mg astrophysical factor. Focusing on the energy region of astrophysical interest around 100 keV, the lowest energy peak was well-fitted with a single resonance centered at 84.3 keV. For this resonance, a strength value was provided for the first time: $1.67 \pm 0.32 \times 10^{-14}$ eV, smaller than the previous upper limit of $\omega\gamma \leq 2.60 \times 10^{-13}$ eV from [23]. The methodology for extracting resonance strengths and their normalization is outlined in [20, 22]. For other resonances below about 300 keV, more stringent upper limits than in [23] were established, while resonance strengths of levels above 300 keV correlated well with those in the literature [23], allowing for a further validation test of the method.

Applying the narrow-resonance approximation and the Monte Carlo method using the `RatesMC` code (check ref.[23] and associated references), we computed the reaction rate, revealing it to be approximately 3 times lower than in [24] at temperatures crucial for the

MgAl cycle. These findings suggest that the MgAl cycle might not close at such temperatures ($T \geq 0.055$ GK), though additional measurements of the ^{27}Al$(p,\gamma)^{28}$Si reaction are necessary. Preliminary astrophysical calculations of AGB star nucleosynthesis indicate that the updated ^{27}Al$(p,\alpha)^{24}$Mg reaction rate enhances ^{27}Al yields in stars experiencing soft hot bottom burning by up to $\sim 25\%$ for solar metallicity in the $4-5\,M_{\odot}$ mass range.

4 Acknowledgements

The author acknowledge the partial support of the European Union - Next Generation EU through the PRIN 2022 project: PRIN_2022RJLWHN, CUP: I53D23000720006

References

[1] Iliadis C. *Nuclear Physics of Stars* (Wiley-VCH Verlag GmbH & Co, Weinheim, 2015)
[2] La Cognata M. et al., Phys. Rev. C **72**, 065802 (2005)
[3] Mukhamedzhanov A.M., et al., Phys. Rev. C. **83**, 044604 (2011)
[4] Tumino A. et al., Annu. Rev. Nucl. Part. Sci. **71**, 345 (2021)
[5] Tumino A. et al., Phys. Lett. B **705**, 546 (2011)
[6] La Cognata M. et al., Phys. Rev. C **80**, 012801 (2009)
[7] Torresi, D., et al., Phys. Rev. C **96**, 044317 (2017)
[8] Pizzone R. G. et al., Eur. Phys. J. A **52**, 24 (2016)
[9] Guardo G. L. et al., Phys. Rev. C **95**, 025807 (2017)
[10] La Cognata M. et al., Astrophys. J. **805**,128 (2015)
[11] Burjan V. et al., Eur. Phys. J. A **55**, 114 (2019)
[12] Trippella O. et al., Astrophys. J. **837**, 41 (2017)
[13] Kiss G.G. et al., Phys. Lett. B **807**, 135606 (2020)
[14] Kiss G.G. et al., Phys. Rev. C **104**, 015807 (2021)
[15] Adelberger E.G. et al., Rev. Mod. Phys. **83**, 195 (2011)
[16] He J.J. et al., Phys. Lett. B **725**, 287 (2013)
[17] Piatti D. et al., Phys. Rev. C **102**, 052802 (2020)
[18] Mukhamedzhanov A.M., et al. Phys. Rev. C **56**, 1302 (1997)
[19] La Cognata M. et al., Astrophys. J. **708**, 796 (2010)
[20] La Cognata M. et al., Astrophys. J. **941**, 96 (2022)
[21] Lamia L. et al., Phys. Rev. C **85**, 025805 (2012)
[22] La Cognata M. et al., Phys. Lett. B **826**, 136917 (2022)
[23] Iliadis C. et al., Nucl. Phys. A **841**, 251 (2010)
[24] Iliadis C. et al., Nucl. Phys. A **841**, 31 (2010)